Available online at www.sciencerepository.org

Science Repository

Research Article

Mechanical properties of 3D bioprinted dermis: characterization and improvement

Mélissa Dussoyer[1], Edwin J. Courtial[1], Marion Albouy[2], Amélie Thépot[2], Morgan Dos Santos[2] and Christophe A. Marquette[1*]

[1]13d.FAB, Univ Lyon, Université Lyon1, CNRS, INSA, CPE-Lyon, ICBMS, UMR 5246, 43, Bd du 11 novembre 1918, 69622 Villeurbanne cedex, France
[2]LabSkin Creations, Edouard Herriot Hospital, 5 place d'Arsonval, Bâtiment 5, 69437, Lyon, France

ARTICLE INFO

Article history:
Received 2 January, 2019
Accepted 16 January, 2019
Published 30 January, 2019

Keywords:
Bioprinting
collagen I
dermis
fibrillin I
mechanobiology
skin

ABSTRACT

Bioprinting is a promising way to create native-equivalent tissues for skin replacement in several pathologies and trauma. These last few years, various constructs have been reported, composed of fibroblasts and keratinocytes used to recapitulate the dermo-epidermal structure. However, the ability to control and characterize the mechanical properties of such constructs is a critical point to insure the transfer of these engineered products to clinic in a near future. In the present study, we had investigated the modulation of the biomechanics of a bioprinted dermis model through physical constrain during tissue maturation. Two passive tension devices were then designed and tested to mature the tissue after printing. Decrease in tissue retraction and increase of collagen I densities, associated to modulations of Young's modulus were obtained after 20 days of tissue maturation. Taken together, these results attest for the first time in literature of promising methods to modulate the mechanical properties of bioprinted skin models.

Introduction

Skin is a complex organ performing many vital functions, from dehydration prevention to protection against external aggressions [1, 2]. It also constitutes a vulnerable structure likely to be altered by various factors [3]. Among the different sources of skin injuries, burns are part of the most common ones. In its last Burns Epidemiology Report, WHO estimated to 11 million the number of people suffering from severe burns and requiring medical attention [4]. Associated with a high morbidity degree, 180 000 deaths annually reported, burns represent a serious global health problem [5, 6]. The restoration of skin integrity and activity in burns victims is still a real challenge since skin substitutes currently used in clinic suffer from difficulties to reproduce the native tissue and to promote its complete regeneration [7].

The democratisation of biological tissues 3D-printing, also called 3D-bioprinting, has revolutionized skin tissue engineering this last decade [8]. Contrary to classic methods, where cells are seeded in the matrix after its production, most bioprinting approaches propose to print tissues already containing skin cells, an interesting time-saving trick [9, 10]. Furthermore, bioprinted-skin production allows a high degree of freedom regarding tissue shape, thickness and cell composition, meaningful advantages in a clinical context promoting personalised medicine [11]. Significant efforts have been invested these last years to develop bioinks made of natural and bioresorbable components which improve the biocompatibility of printed-skins and then promote the autologous regeneration of extracellular matrix during the healing process [12, 13]. To this end, collagen and gelatine were particularly investigated and are now used in most "skin bioinks" [14]. Chitosan was also largely reported as promising additive to modify bioink's rheological properties and promote wound healing in mice [15].

Correspondence to: Christophe A. Marquette, 3d.FAB, Univ Lyon, Université Lyon1, CNRS, INSA, CPE-Lyon, ICBMS, UMR 5246, 43, Bd du 11 novembre 1918, 69622 Villeurbanne cedex, France; E-mail: christophe.marquette@univ-lyon1.fr

http://dx.doi.org/10.31487/j.RGM.2019.01.001

Nowadays, most bioprinted skin-equivalents presented in literature consist in dermo-epidermal structures [16, 17]. These constructs are seeded with human cells, mainly fibroblasts and keratinocytes, and exhibit promising levels of similarity compared to native tissue regarding cellular composition, a fundamental property to insure a satisfying skin replacement [18, 19]. Indeed, the compartmentalisation of dermal and epidermal cells is commonly reached, and the dermal-epidermal junction progressively established after printing [20]. Bioprinted skin mechanics characterization and modulation were however poorly investigated so far, with only seldom works interested in bioinks characterization before cell-seeding and after printing [13]. Among all the published studies dealing with skin bioprinting, none of them ever proposed a rheological characterization of the mature skin substitutes obtained and yet, mechanical properties were reported as largely conditioning the physiology and the integrity of skin [21, 22]. Moreover, reaching mechanical properties allowing the suture of the substitute on patient's native tissue is a key point to insure the compatibility of bioprinted constructions with clinical practices.

Our laboratories recently developed a dermo-epidermal bioprinted skin substitute based on a gelatine-alginate-fibrinogen gel extrusion [19]. This construct reached a cell structuration highly similar to native skin. Complex extracellular matrix components production, testifying of cells viability and functionality in the bioink, were also demonstrated *in vitro* [19]. Deeper characterization of the substitute showed a Young's Modulus of only tens of Pascal, a value largely above the few thousands of Pascal expected in native human skin [23]. A tissue-retraction phenomenon was also observed which was attributed to myofibroblasts development in the dermis.

The present work aims at modulating our bioprinted skin mechanics and retraction through modification of dermis' maturation modalities. Passive constraint was investigated using immobilization devices specifically developed for this goal. Structural and rheological analyses were led to characterize the effects of passive stimulations on bioprinted skin.

Materials and Methods

I Primary human dermal fibroblasts isolation and cultivation

Foreskin samples were obtained from healthy patients undergoing circumcision, according to French regulation including declaration to ministry (DC No. 2014- 2281) and procurement of written informed consent from the patient. Fibroblasts were isolated from 2 years-old donor and cultivated in flasks at 37°C, 5% CO_2 in Dulbecco's modified Eagle medium (DMEM)/Glutamax TM-1 medium (Gibco Cell Culture, Invitrogen, France), supplemented with 10% calf bovine serum (HyClone^{TM}, GE Healthcare Life Sciences, France), 1% penicillin, streptomycin and amphotericine B (Bio Industries-Cliniscience, France). Culture medium was changed every 2 days and cells were routinely passaged in culture flasks until bioprinting. Cells of passages between 7 and 9 were used.

II Bioink formulation and dermis bioprinting

Bioink consisted in a mixture of 10% (w/v) bovine gelatine (Sigma-Aldrich, France), 2% (w/v) fibrinogen (Sigma-Aldrich, France) and 0.5% (w/v) very low viscosity alginate (Alpha Aesar, France) dissolved in NaCl 0.9% (Laboratoire Aguettant, France), as already described [19]. Just before printing, fibroblasts were trypsinized and seeded in the bioink to a concentration of 10^6 cells/mL. Bioink was homogenized and loaded in a sterile 10 mL syringe stored at 37 °C for 15 min for the ink to reach a printable rheology. Pieces of bioprinted dermis 17x17x2 mm (lxLxh) were produced by microextrusion using a specially designed bioprinter (Tobeca, France). Bioprinted dermal pieces were then immerged during 1 h at room temperature in a 0.05% (w/v) thrombin (30-400 NIH/mg, Sigma Aldrich, France) / 3% (w/v) calcium chloride (Sigma Aldrich, France) solution to polymerize fibrinogen and chelate alginate.

III Passive maturation of bioprinted dermis

Maturation devices were modelled using the CAD software SketchUp (Trimble, USA) and produced by photopolymerization of VeroWhite acrylate resin using the Object 30 printer (Stratasys, USA). Devices were washed during 48 h in successive PBS (Gibco Cell Culture, Invitrogen, France) baths in order to eliminate non-polymerized acrylate monomers and photoinitiators. Sterilization of the devices was performed during 24 h by immersion in 70 % ethanol (Gifrer, France). Just before use, sterile structures were rinsed with PBS.

Bioprinted dermis pieces were jabbed on devices (one piece per support) and grown at 37°C, 5% CO_2 atmosphere in (DMEM)/Glutamax TM-1 medium supplemented with 10% calf bovine serum, 1% penicillin, streptomycin and amphotericine B. Medium was changed every 2 days. For each modality, tissues were recovered at days 10 and 20 post-jabbing for retraction measurement, rheological analysis and immunostainings (collagen I and fibrillin I). Bioprinted dermis not jabbed onto the maturation device and cultured in the same conditions was used as a control.

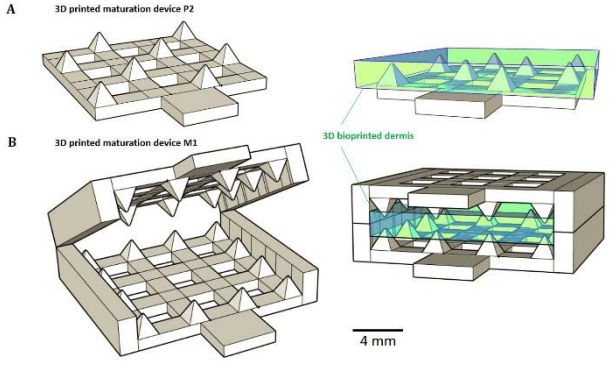

Figure 1. 3D printed passive maturation devices. (A) P2 modality consists in a bottom plate with regularly distributed peaks. (B) M1 system consists in jaws covered with peaks in periphery.

IV Retraction measurement and rheological analysis

For each passive maturation devices, images of fresh living bioprinted dermis were taken immediately before recovering and studied using the software Fiji (NIH, USA) to measure tissues' areas and evaluate retraction. Due to the fragility of bioprinted dermis during cells maturation, we have chosen to use rheological test instead of classic uniaxial tensile test to determine mechanical properties. Rheological analyses of bioprinted dermis matured on passive devices and the control

were performed with a stress controlled DHR-2 rheometer (TA Instruments, USA) using a cross hatched parallel-plate geometry (8 mm). Measurements were performed on living tissues immediately after their recovery, in culture medium maintained at 37 °C. Analysis protocol was performed following a method already described in literature [24]. Briefly, for each tissue, a preliminary study was led to determine its linear viscoelastic domain applying oscillatory stress sweep with a constant frequency. Oscillatory frequency sweep tests were then performed with an angular frequency ranging from 0.1 to 40 rad/s at a constant stress, chosen within the linear viscoelastic domain. At the end of the analysis, the storage modulus *G'* was computed and modelled to determine the experimental Young's modulus E_0 using the following equation[24] (dermis was considered as an incompressible material with a Poisson ratio ν of 0.5):

$$G_0 = \frac{E_0}{2(1+\nu)}$$

where G_0 is the shear modulus.

V Immunofluorescent staining

After 10 and 20 days of total cell culture under passive maturation constrain, bioprinted dermis samples were either immediately cryofixed using OCT compound (VWR International, France) or fixed in formalin 4% and embedded in paraffin.

Collagen I was revealed on 5 µm-thick paraffin slices using anti-collagen I rabbit polyclonal antibody (Novotec, France). Fibrillin I was stained on 12 µm-thick slices of cryofixed tissue with an anti-fibrillin I mouse monoclonal antibody **(**Thermo Scientific, France**)**. All secondary antibody incubations were performed using the appropriated secondary antibody labelled with AlexaFluor 568 (Life Technologies, USA). All fluorescent experiments were coupled by a Hoechst 33342 co-staining **(**Thermo Scientific, France**)** to visualize cells' nuclei. Fluorescence quantifications were performed using Fiji software. Sixteen-bit images were saved in an uncompressed tagged image file format. Six representative images were captured for each condition.

VI Data analysis

Data from retraction measurements, rheological study and fluorescent quantifications were analysed using Rstudio software (R Developers, USA). For studies with replicates higher than 10, normality of samples was first checked using a Shapiro-Wilk test and variance homogeneity verified using a Bartlett Test. One-way analysis of variance (ANOVA) was then performed, followed by Student multiple post-test comparing all pairs. If normality or variances homogeneity was not verified, a multiple non-parametric Wilcoxon test was performed. For studies with sizes per modality equal or lower than 10, a multiple non-parametric Wilcoxon tests was applied. Significant difference was defined as $p<0.05$ and for multiple tests the Bonferroni correction was used to adjust *p* value.

Results

3D bioprinted dermis were produced using our already published method and cultured on specially designed maturation tools [19]. These tools (M1 and P2), which were 3D printed using ink-jet method, are presented in (Figure 1) together with the position of the bioprinted dermis. They were designed in an attempt to obtain dermis passive maturation tools enable to prevent tissue retraction.

Modulations of tissue retraction were observed for tissues grown on M1 and P2 (Figure 1-A), after both 10 and 20 days of total culture. Statistical analyses revealed significant area differences between the 2 tissues and the control at day 10 (Figure 2-A). Control exhibited the smallest area, only 134.1 mm^2, a reduction of a half compared to the initial area of 289.0 mm^2. The largest area was obtained for the tissue peaked on P2 device, with a corresponding area of 256.0 mm^2 against 198.1 mm^2 for the dermis jabbed in M1 device. Retraction phenomenon kept on between days 10 and 20. After day 20, all tissues have lost about half of their initial area. Contrary to day 10, no significant area's difference was detected between maturation modality P2 and M1 at day 20, the tissues exhibiting areas of 116.1 and 117.9 mm^2, respectively. Controls showed a final area of 66.1 mm^2, the equivalent of only 22.2% of the initial area measured immediately after printing. Surfaces of tissues matured on the two types of devices were doubled and significantly different compared to control at day 20. In it worse to note that no significant adhesion phenomenon between tissues material and maturation tools material (acrylate) was observed; recovering of the tissues from the devices was easy and non-destructive to the tissue.

Rheological analyses of mature tissues revealed lower Young's moduli at day 10 for tissues grown on devices compared to control (Figure 2-B). Dermis jabbed in M1 structure exhibited a modulus of 42.6 Pa, less than half of the value obtained for the control. At day 20, all tissues shown an improved stiffness compared to day 10. P2 tissue exhibited the lowest variation of Young's modulus with a final value of 103.3 Pa, the lowest of the 3 modalities. M1 and control tissues exhibited similar elastic moduli of 155.8 and 149.0 Pa. The highest improvement of Young's modulus was observed for M1 dermis with a final value multiplied by 3.7 compared to day 10.

A

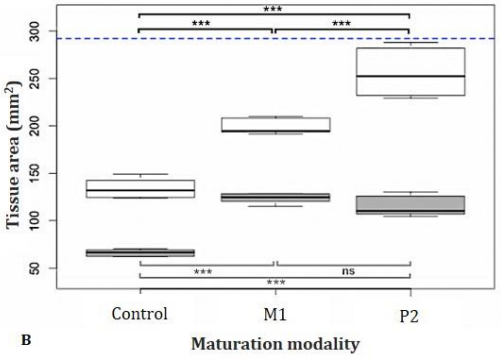

Maturation modality	Young's modulus (Pa)	
	Day 10	Day 20
Control	93.3 ± 2.5	149.0 ± 2.2
M1	42.6 ± 4.0	155.8 ± 4.1
P2	85.1 ± 1.4	103.3 ± 2.5

Figure 2. Bioprinted dermis evolution using passive maturation devices. (A) Retraction analysis after 10 (white boxes) and 20 (grey boxes) days of maturation. Tissues areas were all compared by Wilcoxon tests to determine the significantly different pairs (initial tissue area is

indicated by the blue line, black lines indicate sample's median, n=6). *P < 0.05, **P < 0.01, *** P < 0.001, ns: non-significant. (B) Rheological analysis of bioprinted dermis. Rheometer measurements were performed in triplicate to determine G' and calculate Young's Modulus.

Immunostainings revealed collagen I presence in all tissues at day 10 (data not shown). At day 20, collagen I fibres were homogeneously distributed in the matrix of the two tissues matured on P1 and M2 devices, while they were present only around cells in the control tissue (Figure 3-A). Collagen I network appeared denser in the extracellular matrices of dermis matured on devices than control.

Quantifications of collagen I densities at day 10 revealed higher protein densities in control than in M1 and P2 tissues (Figure 3-B). A mean of 106.7 AU/mm^2 was quantified in control, while M1 and P2 dermis exhibiting densities of 52.8 and 62.7 AU/mm^2, respectively. At day 20, collagen I mean densities in M1 and P2 tissues, i.e. 279.5 and 279.1 AU/mm^2, were significantly different from the 133.7 AU/mm^2 measured in control. Surprisingly, collagen I density in control tissues did not improve a lot during the last 10 days of maturation, while an important increase of 2.5 times was observed for other maturation modalities.

Regarding fibrillin I staining and quantifications, proteins were detected in all tissues at day 20 but no significant difference of densities was observed between the three maturation methods **(*Supporting Information 1*)**.

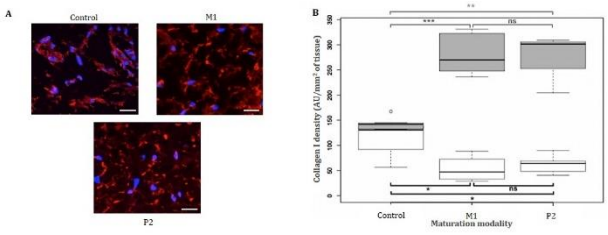

Figure 3. Collagen I immunostaining on matured tissues. (A) Collagen I immunostaining of bioprinted dermis after 20 days of maturation (Blue: Hoechst, red: collagen I, scale bar: 30 µm). Tissues were fixed using a 4% formalin solution, paraffin embedded, cut in 5 µm-thick slices and stained using anti-collagen I monoclonal rabbit antibody. (B) Collagen I immunofluorescent quantification after 10 (white boxes) and 20 (grey boxes) days of maturation. Collagen I densities were all compared by Wilcoxon tests to determine the significantly different pairs (black lines indicate sample's median, n=4). *P < 0.05, **P < 0.01, *** P < 0.001, ns: non-significant

Discussion

Molecular changes happen in bioprinted dermis' extracellular matrix during the maturation phase [25]. Different proteins, mainly secreted by fibroblasts, progressively accumulate and organize to create networks connecting fibroblasts together and to their environment [1]. Collagen I is an early produced marker during dermis growth, while other molecules such as fibrillin, a protein serving as scaffold for elastin dropping on, are deposited later [25]. Connected to cells, collagen and elastin networks are implied in the modulation of mechano-transduction pathways in dermal cells, especially fibroblasts. Surprisingly, none of the publications dealing with skin bioprinting ever studied the modulation of bioprinted skin's mechanics [21]. If molecular skin markers are always stained in tissues to underline their qualitative resemblance to native skin, no data about extracellular matrix proteins densities are given. Regarding retraction, some works evidenced the phenomenon but without any quantification [26]. The devices we developed significantly reduced bioprinted dermis retraction without any strong attachment to a rigid support, but simply in response to the sense of mechanical constraints. Such an observation reinforces the idea that mechanical stimulations can modulate dermal properties.

Regarding molecular evolution, a recent work showed promising results in the field of skin equivalents maturation. In response to a 5-day stretching, improvements of basal membrane components, especially collagens IV and VII, were demonstrated in a human skin equivalent containing keratinocytes and fibroblasts [27]. Our experiment of passive maturation didn't evidenced modification in fibrillin – the pro-elastin network – after growth on devices. As fibrillin production occurs later than collagen, tests of longer maturation durations could provide complementary data to characterize the evolution of this protein. The addition of keratinocytes, epidermal cells previously shown to be implicated in dermal elastin network development, could also promote the production of the protein [28]. We however showed a significant increase in collagen I density after 20 days of maturation, with densities more than doubled compared to control using our devices. Unexpectedly, during the first phase of dermis growth, collagen I secretion seems to be the lowest in tissues under constraints, possibly reflecting an adaptation phase to device's contact, delaying tissue development. Finally, increases of collagen density were observed for all tissues whatever the maturation modality during growth phase. Nevertheless, if at the end of the 20 days maturation, the highest densities correspond to tissues grown on our devices (the less retracted ones), the highest collagen density at day 10 is correlated with the smaller tissue. Thus, no clear correlation between collagen I density and retraction degree can be concluded using the present data. Methods of 3D quantification of immunofluorescence or techniques of genes' transcripts quantification could provide interesting complementary data to complete characterization of collagen I production.

An evolution profile similar to the one observed for collagen I density is observed for Young's modulus, with initial values lower than control and then improving until day 20. The P2 maturation modality is associated to the highest collagen I density and the lowest elastic modulus at day 20. Conversely, at day 10 the highest Young's modulus is associated to the highest collagen I density. Taken together, these data don't suggest any clear correlation between collagen I density and tissue stiffness. However, improvements of Young's modulus occur for all tissues during growth, indicating a progressive gain in stiffness. They finally range between 100 and 155 Pa, values clearly lower than those observed is natural skin. Indeed, even if the elastic modulus evolves from an anatomic region to another and strongly depends on age, values found in literature for native tissue are all about 50 to 100-time higher than in bioprinted skin [23, 29]. In forearm, full-thickness skin Young's moduli were previously estimated to be 101.2, 68.7 and 24.9 kPa for volar, dorsal and palmar regions, respectively. In volar forearm, the elastic modulus of dermis was evaluated to 74 kPa, epidermis and stratum corneum values approaching 100 kPa [23].

Finally, studies of others dermal proteins such as collagens III or V, in addition to longer growth duration allowing the study of elastin, seem necessary to better understand the relations between tissue retraction, tissue mechanics and extracellular matrix composition.

Conclusion

In this study, we have developed and performed the initial evaluation of different *in vitro* methods to maturate bioprinter dermis and modulate its biomechanics and retraction. Using passive maturation systems, we have showed that mechanical properties and molecular composition of our skin model can be modulated in only a few days after printing. Variations in the stiffness of dermis and in collagen I densities were especially noticed in response to static constraints. Altogether, the obtained data suggest promising perspectives for bioprinter skin substitutes engineering and transposition in clinic, once the mechanical properties of the mature tissue strong enough to enable stitching.

Acknowledgment

This work was supported by the French ANR program ASTRID (project BLOC-PRINT - ANR-16-ASTR-0021), led and funded by the Direction Générale de l'Armement (DGA).

References

1. Kolarsick P AJ, Kolarsick MA, Goodwin C (2011) Anatomy and Physiology of the Skin. *J Dermatology Nurses' Association* 3: 203-213.
2. Proksch E, Brandner JM, Jensen JM (2008) The skin: an indispensable barrier. *Exp Dermatol* 17: 1063-1072. [Crossref]
3. Sen CK, Gordillo GM, Roy S, Kirsner R., Lambert L (2009) Human skin wounds: A major and snowballing threat to public health and the economy. *Wound Repair and Regen* 17: 763-771. [Crossref]
4. Peck M D (2011) Epidemiology of burns throughout the world. Part I: Distribution and risk factors. *Burns* 37: 1087-1100. [Crossref]
5. Remo Papin (2004) ABC of burns - Management of burn injuries of various depths. *BMJ* 329: 158-160. [Crossref]
6. Fiona Procter (2010) Rehabilitation of the burn patient. *Indian J Plast Surg* 43(Suppl): S101-113. [Crossref]
7. Halim AS, Khoo TL, Mohd Yussof SJ (2010) Biologic and synthetic skin substitutes: An overview. *Indian J Plast Surg* 43(Suppl): S23-S28. [Crossref]
8. Li J, Chen M, Fan X, Zhou H (2016) Recent advances in bioprinting techniques: approaches, applications and future prospects. *J Transl Med* 14: 271. [Crossref]
9. Murphy SV, Atala A (2014) 3D bioprinting of tissues and organs. *Nat Biotechnol* 32: 773-785. [Crossref]
10. Vijayavenkataraman S, Lu WF, Fuh JY (2016) 3D bioprinting of skin: a state-of-the-art review on modelling, materials, and processes. *Biofabrication* 8(3): 032001. [Crossref]
11. Schork NJ (2015) Personalized medicine: Time for one-person trials. *Nature* 520: 609-611. [Crossref]
12. Kesti M, Muller M, Becher J, Schnabelrauch M, D'Este M, et al. (2015) A versatile bioink for three-dimensional printing of cellular scaffolds based on thermally and photo-triggered tandem gelation. *Acta Biomater* 11: 162-172. [Crossref]
13. Ng WL, Yeong WY, Naing MW (2016) Polyelectrolyte gelatin-chitosan hydrogel optimized for 3D bioprinting in skin tissue engineering. *Int J Bioprinting* 2: 53-62.
14. Ma L, Gao C, Mao Z, Zhou J, Shen J, et al. (2003) Collagen/chitosan porous scaffolds with improved biostability for skin tissue engineering. *Biomaterials* 24: 4833-4841. [Crossref]
15. Dai T, Tanaka M, Huang YY, Hamblin MR (2011) Chitosan preparations for wounds and burns: antimicrobial and wound-healing effect. *Expert Rev Anti Infect Ther* 9: 857-879. [Crossref]
16. Peng He, Junning Zhao, Jiumeng Zhang, Bo Li, Zhiyuan Gou, et al. (2018) Bioprinting of skin constructs for wound healing. *Burns Trauma* 6: 5. [Crossref]
17. Yan WC, Davoodi P, Vijayavenkataraman S, Tian Y, Ng WC (2018) 3D bioprinting of skin tissue: From pre-processing to final product evaluation. *Adv Drug Deliv Rev* 132: 270-295. [Crossref]
18. Michael S, Sorg H, Peck CT, Koch L, Deiwick A (2013) Tissue Engineered Skin Substitutes Created by Laser-Assisted Bioprinting Form Skin-Like Structures in the Dorsal Skin Fold Chamber in Mice. *PLoS ONE* 8: e57741. [Crossref]
19. Pourchet LJ, Thepot A, Albouy M, Courtial EJ, Boher A, et al. (2017) Human Skin 3D Bioprinting Using Scaffold-Free Approach. *Adv Healthc Mater*. [Crossref]
20. Cubo N, Garcia M, Del Cañizo JF, Velasco D, Jorcano JL (2017) 3D bioprinting of functional human skin: production and in vivo analysis. *Biofabrication* 9: 015006. [Crossref]
21. Silver FH, Siperko LM, Seehra GP (2003) Mechanobiology of force transduction in dermal tissue. *Skin Res Technol* 9: 3-23. [Crossref]
22. Wang J, Zhang Y, Zhang N, Wang C, Herrler T, et al. (2015) An updated review of mechanotransduction in skin disorders: transcriptional regulators, ion channels, and microRNAs. *Cell Mol Life Sci* 72: 2091-2106. [Crossref]
23. Liang X, Boppart SA (2010) Biomechanical Properties of In Vivo Human Skin From Dynamic Optical Coherence Elastography. *IEEE Trans Biomed Eng* 57: 953-959. [Crossref]
24. Courtial EJ, Fanton L, Orkisz M, Douek PC, Huet L, et al. (2016) Hyper-Viscoelastic Behavior of Healthy Abdominal Aorta. *Irbm* 37: 158-164.
25. Marcos-Garcés V, Molina Aguilar P, Bea Serrano C, García Bustos V, Benavent Seguí J, et al. (2014) Age-related dermal collagen changes during development, maturation and ageing - a morphometric and comparative study. *J Anat* 225: 98-108. [Crossref]
26. Lee V, Singh G, Trasatti JP, Bjornsson C, Xu X, et al. (2014) Design and fabrication of human skin by three-dimensional bioprinting. *Tissue Eng Part C Methods* 20: 473-484. [Crossref]
27. Tokuyama E, Nagai Y, Takahashi K, Kimata Y, Naruse K (2015) Mechanical Stretch on Human Skin Equivalents Increases the Epidermal Thickness and Develops the Basement Membrane. *PLoS ONE* 10: e0141989. [Crossref]
28. Duplan-Perrat F, Damour O, Montrocher C, Peyrol S, Grenier G, et al. (2000) Keratinocytes influence the maturation and organization of the elastin network in a skin equivalent. *J Invest Dermatol* 114: 365-370. [Crossref]
29. Agache PG, Monneur C, Leveque JL, De Rigal J (1980). Mechanical properties and Young's modulus of human skin in vivo. *Arch Dermatol Res* 269: 221-232. [Crossref]